The indirect antioxidant sulforaphane protects against thiopurine-mediated photooxidative stress

Andrea L.Benedict[1,†], Elena V.Knatko[2,†] and Albena T.Dinkova-Kostova[1,2,*]

[1]Lewis B. and Dorothy Cullman Cancer Chemoprotection Center, Department of Pharmacology and Molecular Sciences, Johns Hopkins University School of Medicine, Baltimore, MD 21205, USA and [2]Jacqui Wood Cancer Centre, Division of Cancer Research, Medical Research Institute, University of Dundee, Dundee DD1 9SY, Scotland, UK

*To whom correspondence should be addressed. Tel. +44-1382-383386; Fax. +44-1382-669993;
Email: a.dinkovakostova@dundee.ac.uk.

Long-term treatment with thiopurines, such as the widely used anticancer, immunosuppressive and anti-inflammatory agent azathioprine, combined with exposure to ultraviolet (UV) radiation is associated with increased oxidative stress, hyperphotosensitivity and high risk for development of aggressive squamous cell carcinomas of the skin. Sulforaphane, an isothiocyanate derived from broccoli, is a potent inducer of endogenous cellular defenses regulated by transcription factor nuclear factor erythroid 2-related factor 2 (Nrf2), including cytoprotective enzymes and glutathione, which in turn act as efficient indirect and direct antioxidants that have long-lasting effects. Treatment with 6-thioguanine, a surrogate for azathioprine, leads to profound sensitization to oxidative stress and glutathione depletion upon exposure to UVA radiation, the damaging effects of which are primarily mediated by generation of reactive oxygen species. The degree of sensitization is greater for irradiation exposures spanning the absorption spectrum of 6-thioguanine, and is dependent on the length of treatment and the level of guanine substitution with 6-thioguanine, suggesting that the 6-thioguanine that is incorporated in genomic DNA is largely responsible for this sensitization. Sulforaphane provides protection against UVA, but not UVB, radiation without affecting the levels of 6-thioguanine incorporation into DNA. The protective effect is lost under conditions of Nrf2 deficiency, implying that it is due to induction of Nrf2-dependent cytoprotective proteins, and that this strategy could provide protection against any potentially photosensitizing drugs that generate electrophilic or reactive oxygen species. Thus, our findings support the development of Nrf2 activators as protectors against drug-mediated photooxidative stress and encourage future clinical trials in populations at high risk for cutaneous photodamage and photocarcinogenesis.

Introduction

Non-melanoma skin cancers are the most common human malignancies. More than 1 million new cases are diagnosed each year in the USA (1). Ultraviolet (UV) radiation is a complete carcinogen and the major causative contributor. Recipients of solid organ transplants are at a remarkably high risk for the development of very aggressive squamous cell carcinomas of the skin: more than 100 times that of the general population (2). Primary preventive measures, such as sunscreens

Abbreviations: CPDs, cyclobutane pyrimidine dimers; DMEM, Dulbecco's modified Eagle's medium; FBS, fetal bovine serum; GSH, glutathione; HBSS, Hank's buffered saline solution; MEF, mouse embryonic fibroblasts; NQO1, NAD(P)H-quinone acceptor oxidoreductase 1; Nrf2, nuclear factor erythroid 2-related factor 2; PBS, phosphate-buffered saline; ROS, reactive oxygen species; SD, standard deviation; SF, sulforaphane (1-isothiocyanato-4R-(methylsulfinyl)butane; 6-TG, 6-thioguanine; UV, ultraviolet.

†These authors contributed equally to this work.

and general sun avoidance, are not sufficiently effective, and new strategies of molecular protection are being explored.

Damage from UV radiation includes direct chemical modification of DNA, generation of reactive oxygen species (ROS) and inflammation (3,4). The solar UV spectrum has two physiologically relevant wavelength components: UVB (280–315 nm) and UVA (315–400 nm) (5). UVB penetrates the epidermis, which consists mainly of differentiated and proliferating keratinocytes (6), damaging DNA directly by promoting cross-linking between DNA bases and also indirectly by causing oxidative stress (4). UVA comprises >95% of the solar UV radiation that reaches the surface of the earth and penetrates into the dermis, reaching the dermal fibroblast population, generating ROS and consequently oxidizing cellular proteins, lipids, polysaccharides and DNA bases (4,6). For recipients of solid organ transplants, the damaging effects of UV radiation are further exacerbated by immunosuppressive therapies. Thus, the thiopurine azathioprine, a commonly used immunosuppressive and anti-inflammatory agent, is a prodrug that is metabolized to 6-thioguanine (6-TG) nucleotide that is incorporated into DNA and RNA (7). Unlike the canonical bases, the 6-TG that is incorporated into DNA absorbs UVA radiation, generating ROS and 6-TG photooxidation products that further damage DNA and proteins, including DNA repair enzymes (8). The combined effects of 6-TG and UVA radiation are therefore not only mutagenic but may also compromise DNA repair. Indeed, the long-term use of azathioprine increases the photosensitivity of the human skin to UVA, but not UVB, radiation (9). Thus, lowering the oxidative stress burden caused by UV radiation is an attractive potential strategy for protection against cell damage that could lead to neoplasia.

Direct antioxidants, such as (–)-epicatechin-3-gallate and carotenoids (i.e. carotenes and lycopene) can protect skin cells from ROS-induced damage (10,11). Their protective effects are short-lived, however, and they are consumed in the process of ROS scavenging (12). An alternative protective strategy is to upregulate the intrinsic antioxidant defenses of cells that comprise phase 2 and antioxidant genes, including those that regulate glutathione (GSH) synthesis, utilization and regeneration (13). The isothiocyanate sulforaphane (SF) that was isolated from broccoli extracts is a potent inducer of these systems (14,15). SF induces cytoprotective enzymes by diverting transcription factor nuclear factor erythroid 2-related factor 2 (Nrf2) from Keap1-mediated proteasomal degradation, resulting in Nrf2 stabilization and promoting nuclear translocation. In the nucleus, Nrf2 binds to the *cis*-acting antioxidant response elements, specific promoter sequences located in the 5′-flanking regions of genes encoding phase 2 and antioxidant cytoprotective proteins. Thus, SF is an *indirect* antioxidant by upregulating cytoprotective proteins and GSH levels. In addition, SF affects multiple processes that contribute to tumor development (16–21). SF suppresses proinflammatory responses, at least partially through inhibition of the NFκB pathway (22), leading to decreased expression of many proinflammatory factors such as inducible nitric oxide synthase, cycloxygenase-2, tumor necrosis factor-alpha and various interleukin cytokines (e.g. IL-1β, IL-6) (23). SF also inactivates the tautomerase activity of the cytokine macrophage migration inhibitory factor (MIF), which may lead to a decrease in the proinflammatory effects of MIF by blocking its interaction with the CD74 receptor on macrophages (24–27). At high concentrations, SF also inhibits phase 1 enzymes, which convert procarcinogens to ultimate carcinogens. Thus, SF inhibits CYP1A1 and 2B1/2 in rat hepatocytes and decreases the activity and transcript levels of CYP3A4 in human hepatocytes (28,29). This ability of SF to upregulate the cytoprotective phase 2 response and to inhibit members of the cytochrome P450 family could ultimately lead to protection against carcinogenesis by inhibiting the activation of procarcinogenic compounds and facilitating their excretion. Microarray analyses of

liver from mice treated orally with SF and of neuroblastoma cells exposed to this isothiocyanate revealed upregulation of subunits of the 26S proteasome (30,31). The heat shock transcription factor 1-mediated heat shock response is also activated by SF, upregulating heat shock proteins 70 (Hsp70) and 27 (Hsp27) and Hsp27-dependent proteasomal activity (32). This regulation of the proteasome and heat shock response may indicate that SF-mediated protection against oxidative stress and cellular injury may be partially due to removal of damaged proteins.

SF can also influence tumor formation through its ability to cause cell cycle arrest by regulating the expression of various cyclins, cyclin-dependent kinases (CDK), CDK inhibitors and other cell cycle-related genes (reviewed in refs 20 and 23), or by disrupting microtubule formation via inhibition of tubulin polymerization (33,34). Another potential mediator of the anticarcinogenic effects of SF is inhibition of histone deacetylases (HDACs). SF downregulates histone deacetylase activity and increases acetylated histones bound to the *p21* promoter, which regulates cyclin-dependent cell cycle progression (35). Apoptotic effects of SF have been observed in many different cancer cell lines. In these cases, SF treatment resulted in downregulation of antiapoptotic Bcl-2 and Bcl-XL, upregulation of proapoptotic Bax and activation of caspase-3 (36). There is also evidence that SF can decrease both angiogenesis and metastasis, by inhibiting the expression of the proangiogenic factors, vascular endothelial growth factor, hypoxia-inducible factor-1 alpha, c-Myc and suppressing matrix metalloproteinase-2, which affects basement membrane integrity and promotes metastasis (37).

Studies in Nrf2-knockout mice have shown that oxidative DNA damage and inflammation in ear skin tissue is increased with chronic UVB exposure as compared with damage in wild-type mice (38). In addition, Nrf2 has been implicated in the protective effect of quercetin against UVA-induced oxidative stress and apoptosis in the human keratinocyte cell line HaCaT (39). These findings suggest that the Nrf2 pathway plays an important role in protection against UV insult and that SF-mediated upregulation of this pathway could reduce oxidative DNA damage and inflammation induced by UV radiation. SF protects mouse and human keratinocytes against oxidative stress caused by chemical oxidants and UVA radiation (16,40). Recently, the indirect antioxidant effect of SF was also observed in 6-TG-treated murine hepatoma (Hepa1c1c7) cells challenged with UVA radiation (41). However, to our knowledge, the potential protective effect of SF and its dependence on either Nrf2 or solar spectrum wavelength have not been investigated in primary skin cells exposed to the combination of 6-TG and UVA radiation. This is important because the combination of 6-TG and UVA radiation is carcinogenic to the skin largely due to damage of DNA and associated proteins caused by ROS and the subsequent formation of 6-TG photooxidation products. Furthermore, as SF treatment of hepatoma cells decreases the incorporation of 6-TG in DNA (41), it is necessary to determine whether protection by SF could be achieved under conditions of identical 6-TG DNA levels. As photooxidative stress constitutes the initial event causing damage to DNA, proteins and lipids, which may ultimately lead to carcinogenesis, in this study, we asked whether SF protects primary dermal fibroblasts and keratinocytes isolated from SKH-1 hairless mice against oxidative stress caused by UVA radiation under basal conditions as well as after treatment with the thiopurine 6-TG. This information is critical for the design of future chemoprevention studies in high-risk populations for the development of skin cancer, such as organ transplant recipients or inflammatory bowel disease patients who are undergoing chronic, often life-long, thiopurine therapies.

Materials and methods

Cell cultures

All procedures were performed in accordance with the regulations described in the UK Animals (Scientific Procedures) Act 1986. SKH-1 hairless mice, initially obtained from Charles River (Germany), were bred in our facility. The animals were kept on a 12 h light/12 h dark cycle, 35% humidity and had *ad libitum* access to water and food (pelleted RM1 diet that was purchased from

SDS Ltd, Witham, Essex, UK). To isolate primary keratinocytes and dermal fibroblasts, skins were removed from 2-day-old pups and floated, dermis-side down, on 0.25% trypsin (without ethylenediaminetetraacetic acid) (Gibco) overnight at 4°C (42). The dermis was separated from the epidermis, cut into small pieces and incubated at 37°C for 1–2 h in high-glucose Dulbecco's modified Eagle's medium (DMEM) containing 0.35% collagenase type I (Gibco) with gentle agitation every 10 min. Dissociated cells were collected by centrifugation at 1200 r.p.m. for 5 min at 25°C, resuspended in complete dermal fibroblast medium [high-glucose DMEM, 10% fetal bovine serum (FBS) and 1% Pen/Strep] and centrifuged at 1200 r.p.m. for 5 min at 25°C. Cells were suspended in complete dermal fibroblast medium, plated in 10-cm plates, and maintained in 5% CO_2 at 37°C. Within two passages (splitting cells 1:10 every 3 days) the dermal fibroblast culture was >95% pure, as assessed by immunostaining for markers of dermal fibroblasts (vimentin, mouse, clone V9; Sigma–Aldrich) and keratinocytes (keratin 17, a kind gift of Pierre Coulombe, Johns Hopkins University). Once purity was established, dermal fibroblasts were plated at passage 3–4 in 6-well plates for experiments.

For primary keratinocyte isolation, cells were removed from the epidermis using a cell scraper and suspended in cold low glucose DMEM medium (Gibco). Cells were centrifuged at 1200 r.p.m. for 5 min at 4°C, resuspended in cold low glucose DMEM medium, carefully overlaid on Lymphoprep (Axis-Shield PoC AS) and centrifuged at 1800 r.p.m. for 30 min at 4°C. Keratinocytes were collected from the interface between the medium and Lymphoprep solution. Fresh DMEM was added, and the cells were pelleted by centrifugation at 4°C. Keratinocytes were then resuspended in MKer medium [three parts low glucose DMEM medium, one part Ham's F-12 medium (Gibco), 10% FBS (Biowhitaker), 60 µg/ml penicillin (Sigma), 25 µg/ml gentamicin (Sigma), 5 µg/ml insulin (Sigma), 0.4 µg/ml hydrocortisone (Sigma), 5 µg/ml transferrin, 2.0 pM 3,3-5′-triiodo-L-thyroxine (Sigma), 0.1 pM cholera toxin (ICN), 10 ng/ml epidermal growth factor (Sigma)], and immediately plated in 6-well plates for experiments. Kera-308 murine keratinocytes, obtained from Cell Lines Service (Eppelheim, Germany), were grown in Minimum Essential Medium (Eagle) supplemented with 10% (vol/vol) heat-inactivated FBS, 1% (vol/vol) non-essential amino acids and 2 mM L-glutamine.

Mouse embryonic fibroblasts (MEFs), originally isolated from 13.5-day-old embryos of wild-type or Nrf2-knockout C57BL/6 mice, were cultured in plastic dishes coated for 30 min with 0.1% (wt/vol) gelatin before use. The cell culture medium was Iscoves Modified Dulbecco's Medium (with L-glutamine) supplemented with human recombinant epidermal growth factor (10 ng/ml), 1 × insulin/transferrin/selenium and 10% (vol/vol) heat-inactivated FBS, all from Invitrogen. Cell cultures were maintained in 5% CO_2 at 37°C.

UVB irradiation and detection of cyclobutane pyrimidine dimers and 6,4 pyrimidine–pyrimidone photoproducts

Cells (250 000 per well) were grown for 24 h on 0.1% gelatin-coated glass cover slips placed on the bottom of the wells of 6-well plates. Cells were treated with solvent control (0.1% acetonitrile, vol/vol) or SF (1.0 µM) for a further 24 h. The cell culture medium was then removed; the cells were washed twice with phosphate-buffered saline (PBS) and exposed to UVB radiation (20 mJ/cm²) in 1 ml of Hank's balanced salt solution (HBSS). UVB radiation was provided by broadband (280–320 nm) UVB lamps (FS72T12-UVB-HO, National Biological Corporation, Twinsburg, OH). The radiant dose was quantified with a UVB Daavlin Flex Control Integrating Dosimeter and further calibrated with an external radiometer (X-96 Irradiance Meter; Daavlin, Bryan, OH). Control cells were sham-irradiated (the plates were wrapped in aluminium foil to shield them from the UV radiation) and placed under the UV lamps alongside the radiated cells. After irradiation, cells were incubated in 5% CO_2 at 37°C for the indicated periods of time before being fixed and processed for immunodetection of cyclobutane pyrimidine dimers (CPDs) and 6,4 pyrimidine–pyrimidone photoproducts (6,4-PPs). For immunostaining, cells were permeabilized with 0.5% Triton X-100 in PBS for 5 min on ice and washed with PBS. Cells were treated with 2 M HCl at room temperature for 30 min to denature the nuclear DNA. After washing with PBS, cells where incubated with 20% normal goat serum in PBS at 37°C, with gentle shaking, for 30 min. Cells were washed with PBS and then incubated with primary antibodies to CPDs (1:1000 dilution) (clone TDM-2; MBL Co., LTD, Japan) and 6,4-PPs (1:400 dilution) (clone 64M-2; MBL Co., LTD, Japan) in 5% normal goat serum in PBS for 1 h at 37°C with gentle shaking. After washing with PBS, cells were incubated with fluorescein isothiocyanate-conjugated secondary antibody (1:200 dilution) (goat antimouse fluorescein isothiocyanate; KPL, Inc, Gathersburg, MD in 5% normal goat serum in PBS for 30 min at 37°C with gentle shaking. Cells were washed with PBS and nuclei were stained with 4′,6-diamidino-2-phenylindole. Coverslips were mounted on slides using Vectamount medium (Biomedia). Fluorescent images were recorded using a Zeiss AxioPlan2 upright microscope equipped with a Zeiss HRC high-resolution digital camera (Thornwood, NY).

UVA irradiation, and determination of ROS, GSH and NAD(P)H-quinone acceptor oxidoreductase 1 levels

Cells (200 000 per well) were grown in 0.1% gelatin-coated 6-well plates for 24 h. Cells were treated with solvent control (0.1% acetonitrile, vol/vol) or SF for 24 h. For experiments with 6-TG, cells were treated with SF for 24 h before exposure to 6-TG (Sigma–Aldrich Co, Poole, Dorset, UK). For determination of ROS, cells were washed with PBS and loaded with 1 ml of 10 μM 2′,7′-dichloro-dihydrofluorescein diacetate (Invitrogen Ltd, Paisley, UK) in HBSS for 30 min at 37°C, then washed twice with HBSS, covered with 1 ml of HBSS, and exposed to UV radiation. Control cells were sham-irradiated (wrapped in aluminium foil to shield them from the UV radiation) and placed under the UV lamps for the same exposure time as the highest dose of UV radiation. Cells were irradiated with a Dermalight Ultra 1 UVA-1 spectrum lamp (340–400 nm, Dr Hönle UV Technology, Gräfelfing, Germany) or with broadband spectrum UVA PUVA lamps (320–420 nm). The irradiance at the surface of the cells, at a distance of 330 mm from the lamps, was measured with a Waldmann UV meter calibrated to each radiation source by use of a double-grating spectroradiometer (Bentham Instruments Ltd, Reading, UK). Any UVB component from the radiation sources (<0.05%) was filtered out by a 7 mm thick glass plate. When exposed to UVA-1 radiation, cells were placed on top of an ice-chilled metal pan to avoid overheating. During exposure to UVA radiation, cells were kept at room temperature as the amount of heat that is generated by these radiation sources is negligible.

Generation of ROS was quantified 1 h postirradiation by the fluorescence intensity of the oxidized probe by using a microtiter plate reader with excitation at 485 nm and emission at 530 nm. Reduced glutathione was determined by incubating irradiated cells with 40 μM monochlorobimane for 1 h at 25°C; formation of the GS-monochlorobimane adduct was quantified in live cells 2 h after irradiation by using the same microtiter plate reader with excitation at 390 nm and emission at 490 nm. PBS was then removed and 150–300 μl of 0.08% digitonin, 2 mM ethylenediaminetetraacetic acid, pH 7.8, were added to each well and incubated at 37°C for 30 min. Cell lysates were transferred to a 96-well plate for determination of NAD(P)H-quinone acceptor oxidoreductase 1 (NQO1) enzyme activity by the Prochaska test (43,44) and protein concentration by the bicinchoninic acid assay (Thermo Scientific, Rockford, IL).

Determination of 6-thioguanine incorporation into DNA

MEFs (1.5×10^6 per dish) were plated on 10-cm dishes. Twenty-four hours later, the medium was removed and the cells were exposed to 6-TG for a further 24 h. The incorporation of 6-TG nucleotide into DNA was quantified after its stoichiometric oxidative conversion to the fluorescent product guanine sulfonate deoxyriboside (GSO_3dR) (41,45). DNA was extracted from cells, oxidized with magnesium bis(monoperoxyphthalate) in the dark for 30 min at room temperature, and ethanol-precipitated. Following denaturation by heating at 90°C for
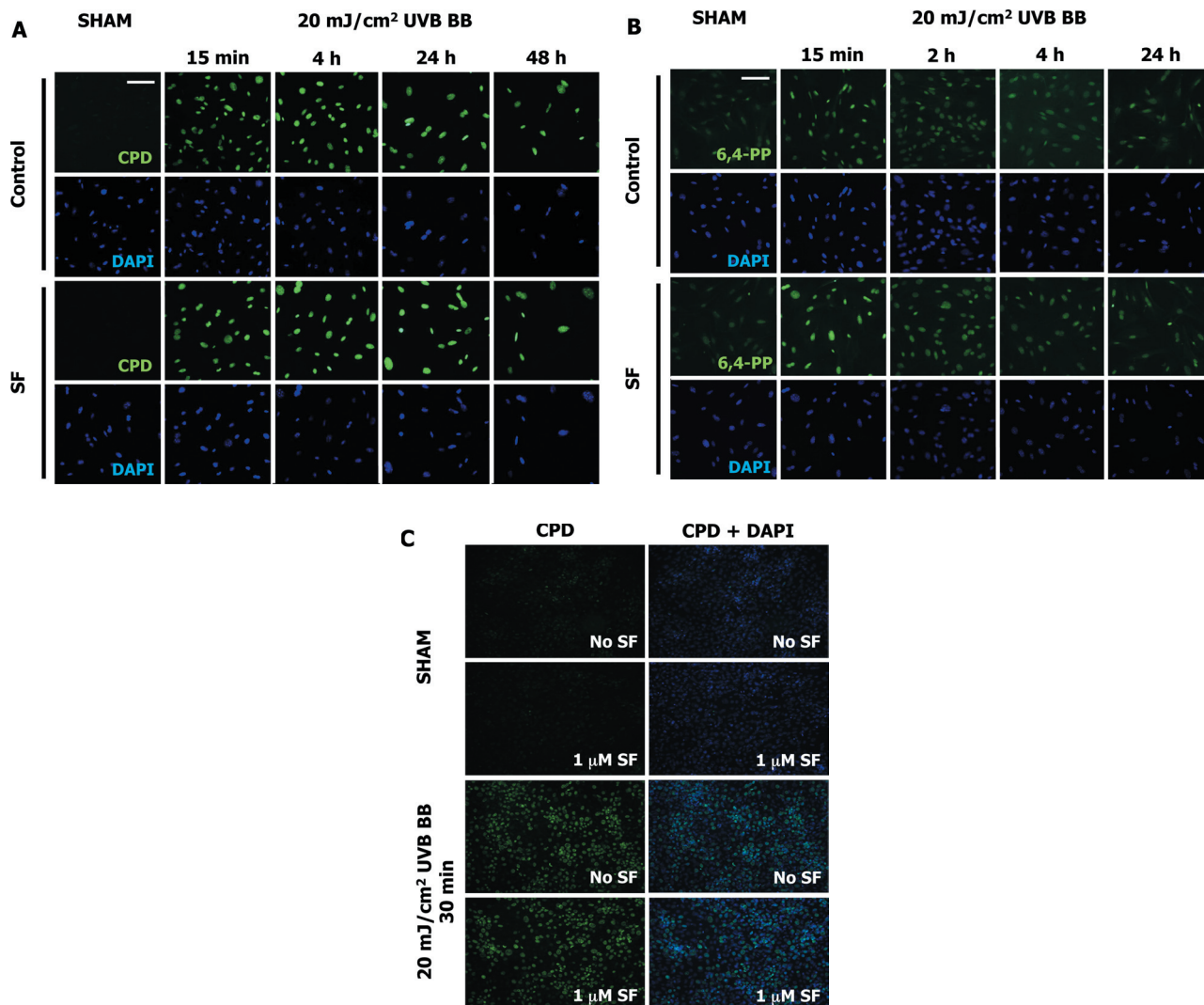

Fig. 1. Sulforaphane does not affect the formation of DNA photoproducts caused by UVB radiation. Primary SKH-1 dermal fibroblasts (250 000 cells per well; **A** and **B**) or keratinocytes (500 000 cells per well; **C**) were plated in 6-well plates. Cells were treated with either solvent (0.1% acetonitrile) or 1 μM SF for 24 h. Cells were then exposed to 20 mJ/cm² of broadband UVB radiation. Control cells were sham-irradiated (wrapped in foil) and left under the UV lamps for the same exposure time. Cells were fixed at the indicated times and immunostained for CPDs or 6,4-PPs. CPDs (A and C) and 6,4-PPs (B) were detected in the nuclei of both control and SF-treated cells at different time points after UV exposure. No difference between control and SF-treated cells were observed with sham exposure or at any time point following UV irradiation for both CPDs (A and C) and 6,4-PPs (B). Scale bar: 100 μm.
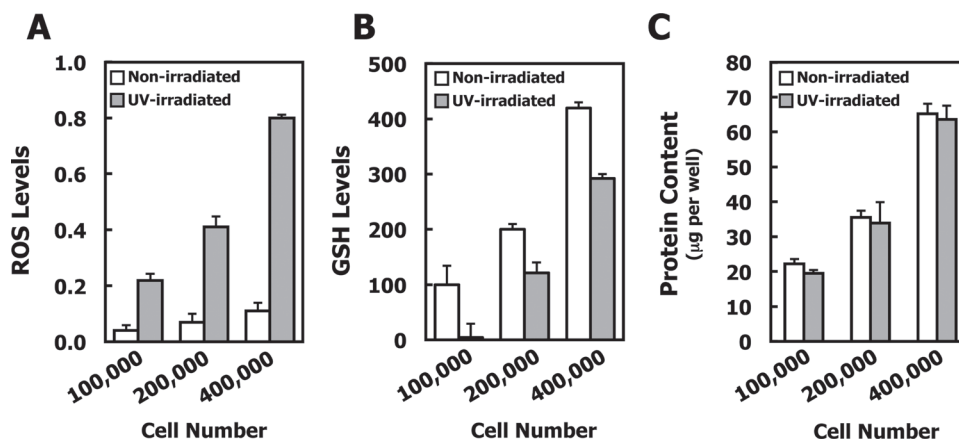
Fig. 2. Exposure to UVA radiation causes oxidative stress and depletion of GSH. Primary SKH-1 dermal fibroblasts were plated (100 000, 200 000 and 400 000 per well) in 6-well plates and irradiated with 15 J/cm^2 UVA-1 48 h after plating. The non-irradiated control plates were wrapped in foil and placed under the lamps adjacent to the irradiated plates. (**A**) ROS levels were detected by the fluorescent probe 2′,7′-dichlorodihydrofluorescein diacetate diacetate (excitation: 485 nm/emission: 530 nm), 1 h after irradiation. (**B**) GSH levels were determined with monochlorobimane. The GS-monochlorobimane conjugate was quantified by fluorescence (excitation: 390 nm/emission: 490 nm) and expressed at the percentage of non-irradiated control cells. $P < 0.001$ for all data points when non-irradiated cells are compared with irradiated cells. (**C**) Protein content per well showing a proportional increase in protein with increasing cell density, with no UV radiation-induced differences in protein content at any cell density. For all panels, mean ± SD are shown ($n = 3$). Results are representative of three different experiments.

5 min, DNA (120 µg) was cooled on ice, and digested with 24 units nuclease P1 (1 U/µl) for 1 h at 50°C. The pH was then adjusted to 8.0 with 20 µl of 1 M Tris-Cl buffer (pH 8.0), and the sample was incubated with alkaline phosphatase (2 units) for 1 h at 37°C. The resulting deoxynucleosides were separated by reverse phase high-performance liquid chromatography on Ascentis C18 columns (Supelco, 250×4.6 mm, 5 µm) with use of an Agilent 1100 system equipped with Agilent G1314A variable wavelength detector and Agilent G1321A fluorescence detector. A standard curve was constructed using a 30mer single-stranded oligodeoxyribonucleotide (originally a kind gift from Peter Karran, Cancer Research, UK, and thereafter obtained from Oligo Etc., Wilsonville, OR) which contained one 6-TG and four Gs, after oxidation with magnesium bis(monoperoxyphthalate), digestion with nuclease P1, and treatment with alkaline phosphatase. The deoxynucleosides were eluted at a constant flow rate of 0.5 ml/min, with a gradient initially from 10 mM KH$_2$PO$_4$ (pH 6.7) to 10% CH$_3$OH (0–10 min), and subsequently from 10 to 40% CH$_3$OH (10–20 min) in the same buffer. The amount of guanine sulfonate deoxyriboside was quantified by fluorescence (excitation at 320 nm/emission at 410 nm). The dG content of the same sample was determined by absorbance at 260 nm after 1:20 dilution.

Western blotting

For western blot analysis of the levels of Nrf2, MEFs (1.5 × 10^6 per dish) were grown for 24 h in 10 cm dishes. Cells were treated with 3 µM SF for a further 3 h, washed 3 times with Dulbecco's phosphate-buffered saline, and lysed in radioimmunoprecipitation assay buffer (50 mM Tris-HCl, pH 7.5; 150 mM NaCl; 1% NP-40; 0.5% sodium deoxycholate; 0.1% sodium dodecyl sulfate; 1 mM ethylenediaminetetraacetic acid) on ice for 30 min. Proteins were subjected to electrophoresis on a 10% sodium dodecyl sulfate–polyacrylamide gel electrophoresis and then electrophoretically transferred to immobilon-P membrane (Millipore, Watford, Herts., UK). After blocking with 10% non-fat milk at 4°C for 2 h, immunoblotting was performed using a rabbit monoclonal antibody (a kind gift from John D. Hayes, University of Dundee) at a dilution of 1:2000 (46). The antibody against glyceraldehyde-3-phosphate dehydrogenase (Sigma–Aldrich Co., 1:5000 dilution) was used as a loading control.

Statistical analysis

All values are mean ± 1 SD (standard deviation). The differences between groups were determined by Student's *t*-test.

Results and discussion

Sulforaphane protects primary dermal fibroblasts and keratinocytes against oxidative stress caused by UVA-1 radiation

We first examined the damaging effects of UV radiation on primary SKH-1 dermal fibroblasts. Exposure to broadband UVB (280–320 nm, 20 mJ/cm^2) radiation caused direct DNA damage as evidenced by the formation of CPDs and 6,4-PPs (Figure 1A and 1B).

Both types of DNA photoproducts were readily detectable 15 min after irradiation, the earliest time point examined, and then decreased by 24–48 h, suggesting the occurrence of repair processes and/or cell death. Nuclear (4′,6-diamidino-2-phenylindole) staining in both control and SF-treated cells at all time points observed after UV exposure showed co-staining for DNA damage markers (CPD and 6,4-PPs). Under these experimental conditions, treatment with SF for 24 h before exposure to UVB had no significant effect on the extent of either of these two types of direct DNA damage (Figure 1A and 1B). Additional experiments in primary SKH-1 keratinocytes confirmed this finding (Figure 1C).

To examine the effects of UVA radiation, initially we chose the UVA-1 Dermalight Ultra 1 lamp (340–400 nm) for the radiation source. The use of this lamp has the advantage of a higher power output than traditional UVA sources, thereby reducing the exposure time needed to deliver a desired UVA dose. To determine whether UVA-1 radiation causes oxidative stress, dermal fibroblasts were exposed to UVA-1 (15 J/cm^2) and the levels of ROS and GSH were determined. The changes in the levels of ROS and GSH were proportional to the number of cells (Figure 2A and 2B). Compared with non-radiated control cells, UVA-1 radiation resulted in a striking ~8-fold increase in ROS levels and decreased GSH by ~40% when cells were plated at a cell density of 200 000 cells per well 48 h before radiation. The protein concentrations of the cell lysates were proportional to the cell number, with no differences between non-radiated and radiated plates (Figure 2C).

The levels of ROS were dependent on the dose of UVA-1 radiation (Figure 3A, open symbols), and were markedly lower in cells that had been treated with 1 µM SF for 24 h before radiation (Figure 3A, closed symbols). SF treatment resulted in increased synthesis of GSH such that, even at the highest dose of UVA-1 (20 J/cm^2), the GSH levels were only slightly lower than the basal levels of GSH in sham-irradiated control cells (Figure 3B). The NQO1 enzyme activity was enhanced by ~3-fold upon SF treatment (Figure 3C). Interestingly, UVA-1 exposure caused a slight elevation in NQO1 activity, in agreement with a study by Hirota and colleagues (47) who found that UVA radiation activated the Nrf2 pathway and that treatment with hematoporphyrin, a photosensitizer that generates ROS, before UV exposure, increased Nrf2 nuclear accumulation.

Like dermal fibroblasts, primary keratinocytes also showed large, dose-dependent responses to UVA-1 irradiation (Figure 3D, open symbols), with dramatic reduction in GSH levels when irradiated
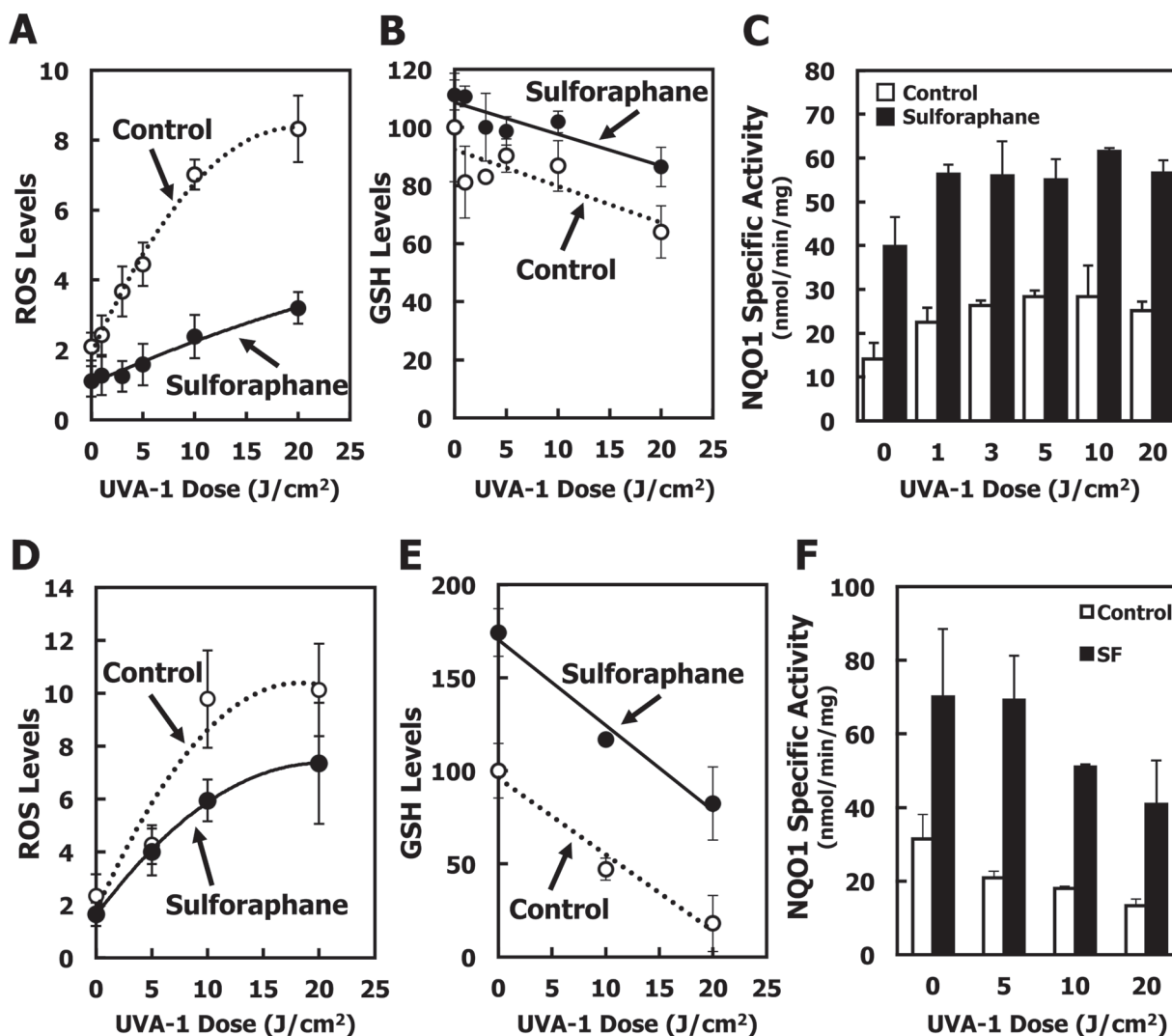
Fig. 3. Sulforaphane induces NQO1 and protects against UV radiation-induced ROS formation. Primary SKH-1 dermal fibroblasts (**A–C**) or keratinocytes (**D–F**) were plated at 200 000 cells per well in 6-well plates. Cells were treated with either solvent (0.1% acetonitrile) (open symbols) or 1 µM SF (closed symbols) for 24 h. After loading with 2′,7′-dichlorodihydrofluorescein diacetate, cells were exposed to UV radiation. Control cells were sham-irradiated (wrapped in foil) and left under the UV lamps for the same exposure time as the highest dose of UV radiation. (A and D) Fluorescence intensity of the ROS probe was measured (excitation: 485 nm/emission: 530 nm) 1 h after irradiation, and normalized to protein concentration. (B and E) GSH was measured by fluorescence of the GS-monochlorobimane conjugate (excitation: 390 nm/emission: 490 nm) 2 h after irradiation, normalized to protein concentration, and expressed as the percentage of non-irradiated, solvent-treated cells. (C and F) NQO1 enzyme activity was measured 2 h after UV radiation.). *P* < 0.01 for all data points when SF-treated cells are compared with control (acetonitrile solvent-treated) cells with the exception of the levels of ROS at the lowest and the highest UV dose for which the differences were not statistically significant. Results are representative of three different experiments.

with 20 J/cm² UVA-1 (Figure 3E, open symbols). Although to a much smaller extent in comparison with dermal fibroblasts, the protective effect of SF was also evident in these cells (Figure 3D and 3E, closed symbols). The lower magnitude of protection is most probably due to the greater depletion of GSH, which was by ~82% in keratinocytes at 20 J/cm² UVA-1 (Figure 3E, open symbols) compared with the much smaller ~36% depletion in GSH levels in dermal fibroblasts (Figure 3B, open symbols). Interestingly, although UVA exposure did not affect the ability of either cell type to induce NQO1 upon SF treatment, in keratinocyte cultures we observed an overall reduction of NQO1 activity with increasing UVA dose (Figure 3F), in contrast with dermal fibroblasts which showed a slight elevation of NQO1 activity with increasing UVA exposure (Figure 3C). Since keratinocytes had a more severe depletion in GSH levels upon UVA irradiation than dermal fibroblasts, this effect on NQO1 enzyme activity probably reflects the occurrence of overall oxidative damage, which leads to a depression of NQO1 activity.

Sulforaphane protects 6-thioguanine-treated primary dermal fibroblasts against the damaging effects of UVA-1 radiation

We next asked whether SF could protect dermal fibroblasts that were also exposed to the thiopurine 6-TG, against oxidative stress caused by UVA radiation. When cells were first treated for 24 h with 6-TG and then exposed to UVA-1 radiation, the levels of ROS were increased by 2-fold compared with the ROS levels in cells that were irradiated but not treated with 6-TG, demonstrating that 6-TG sensitizes the cells to oxidative stress (Figure 4A, gray bars). The degree of this sensitization effect depended on the duration of exposure to 6-TG, and was further increased to 4-fold after exposure to 6-TG for 48 h. An independent experiment (by use of cell counting) established that, under these experimental conditions, the doubling time of primary dermal fibroblasts is ~24 h. Importantly, the dependence of the sensitization to oxidative stress on the time of exposure to 6-TG (and consequently on the number of cell divisions) strongly suggests that the sensitization is largely determined by the amount of 6-TG that is incorporated in the DNA, rather than by the free drug that is present in the cell.
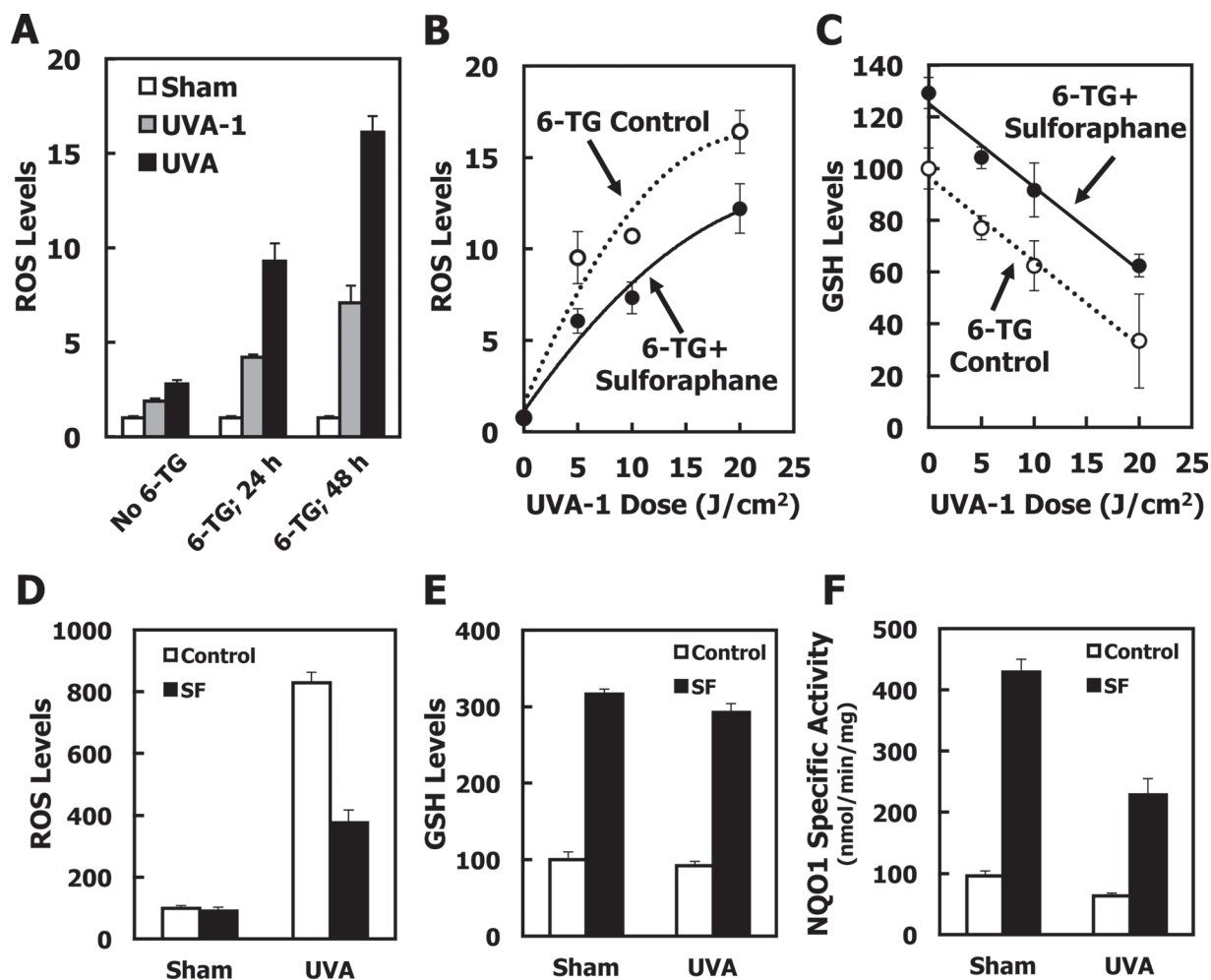
Fig. 4. Sulforaphane protects 6-TG-treated dermal fibroblast and keratinocytes against UV radiation-induced ROS formation and GSH depletion. (**A**) Primary SKH-1 dermal fibroblasts were plated at 120 000 cells per well in 6-well plates. After 24 h, they were treated with either solvent (0.00005 N NaOH) or 1 μM 6-TG for a further 24 or 48 h. Cells were then washed with HBSS, and exposed to UVA-1 (3 J/cm², gray bars) or UVA (3 J/cm², black bars) radiation in 1.0 ml of HBSS. ROS generated by the UV radiation were quantified by the probe 2′,7′-dichlorodihydrofluorescein diacetate and fluorescence intensity was measured 1 h postirradiation. (**B** and **C**) Cells were plated at 200 000 cells per well in 6-well plates. After 24 h, they were treated with either solvent (0.1% acetonitrile, white symbols) or 2 μM SF (black symbols) for 24 h. The medium was then changed to fresh medium that, in addition to 2 μM SF, also contained 1 μM 6-TG, and the cells were incubated for a further 48 h. Cells were then exposed to UVA-1. ROS, normalized to protein (B), and GSH, normalized to protein and expressed as the percentage of non-irradiated, solvent-treated cells (C), were determined 1- and 2 h after irradiation, respectively. (**D–F**) Kera-308 murine keratinocytes (250 000 per well) were plated on 6-well plates. Following incubation overnight, they were treated with either vehicle (0.1% acetonitrile, white bars), or 5 μM SF (black bars) for 24 h. The medium was removed, and the cells were then exposed to either vehicle (0.00005 N NaOH) or 0.5 μM 6-TG for a further 24 h. After loading with 2′,7′-dichlorodihydrofluorescein diacetate, the cells were washed with HBSS and exposed to UVA (3 J/cm²) in 1.0 ml of HBSS. ROS, normalized to protein (D), and GSH, normalized to protein and expressed as the percentage of non-irradiated, solvent-treated cells (E), were determined 1- and 2 h after irradiation, respectively. The specific activity of NQO1 (F) was measured in cell lysates and is expressed as a ratio to the activity of sham-irradiated control cells. For all panels, mean ± SD are shown ($n = 3$). $P < 0.01$ for all data points when treated cells are compared with control cells. Results are representative of three independent experiments.

When cells were treated with SF for 24 h, then co-treated with SF and 6-TG for a further 48 h, and finally exposed to UVA-1 radiation, there was a significant ~30% reduction in the formation of ROS in comparison with cells that had not been treated with SF (Figure 4B). Similar to the experiment in the absence of 6-TG (Figure 3B), SF treatment also increased the levels of GSH in the presence of 6-TG (Figure 4C). In agreement with the higher ROS levels in cells treated with 6-TG than in cells that had not been treated with 6-TG (Figure 4A), GSH depletion was accelerated in 6-TG-treated cells (compare Figure 4C and Figure 3B). Although depletion of GSH still occurred in response to radiation exposure, independently of SF treatment, at all doses of UVA-1 the levels of GSH were higher in SF-treated cells than in control cells. Thus, the protective effects of SF against oxidative stress caused by UV radiation were evident under both basal conditions and after thiopurine treatment.

Sensitization to UVA-mediated oxidative stress in 6-thioguanine-treated cells is causatively related to the absorption properties of 6-thioguanine

To further confirm the causative role of 6-TG for the sensitization to UVA radiation-mediated oxidative stress, we used a broadband UVA radiation source. In contrast with the UVA-1 radiation source emitting in the 'long' UVA-1 region (i.e. 340–400 nm) where 6-TG absorbs only partially, the broadband UVA radiation source has an emission spectrum (320–420 nm) that encompasses almost the entire absorption spectrum (300–370 nm, λ_{max} = 340 nm) of 6-TG in the UVA region (7). As predicted, under conditions of broadband UVA radiation, the 6-TG sensitization to oxidative stress was greater than in 6-TG-treated UVA-1 irradiated cells (Figure 4A, compare gray and black bars). Consistent with the UVA-1 radiation experiments (Figure 4A, gray bars), the degree of the sensitization effect to broadband UVA radiation depended on the
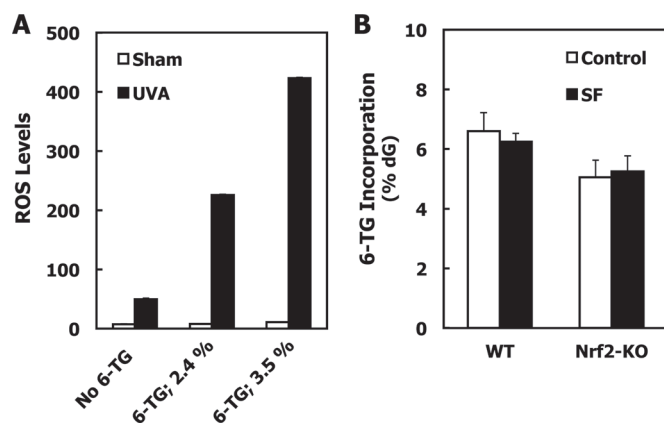
Fig. 5. Sulforaphane treatment of MEFs does not alter the extent of incorporation of 6-TG into their genomic DNA. (**A**) Wild-type MEFs were plated at 250 000 cells per well in 6-well plates. After 24 h, they were treated with either vehicle (0.00005 N NaOH) or 6-TG for a further 24 h. Cells were then washed with HBSS, and exposed to UVA (3 J/cm^2) radiation in 1.0 ml of HBSS. ROS generated by the UV radiation were quantified by the probe 2′,7′-dichlorodihydrofluorescein diacetate and fluorescence intensity was measured 45 min postirradiation. The incorporation of 6-TG in genomic DNA was quantified in a parallel experiment by the fluorescence of guanine sulfonate deoxyriboside following DNA extraction, oxidation, digestion and high-performance liquid chromatography separation. Mean ± SD are shown ($n = 3$). (**B**) MEFs (1.5×10^6 per dish) were plated on 10-cm dishes. Seven hours later, they were treated with either vehicle (0.1% acetonitrile, white bars), or 3 µM SF (black bars) for 17 h. The medium was removed, and the cells were then exposed to 6-TG (1 µM for wild-type or 0.5 µM for Nrf2-knockout MEFs) for a further 24 h. The incorporation of 6-TG in genomic DNA was quantified as described in (A). Mean ± SD are shown ($n = 3$). Results are representative of three different experiments. WT, wild-type and Nrf2-KO, Nrf2-knockout cells.

duration of exposure to 6-TG, and the levels of ROS were increased by 3- and 6-fold for cells that were exposed to 6-TG for 24- and 48 h, respectively, compared with the ROS levels in cells that were irradiated but not treated with 6-TG (Figure 4A, black bars). Taken together, these results demonstrate that the degree of sensitization is (i) greater for radiation exposures that span the absorption spectrum of 6-TG, and (ii) proportional to the number of cell divisions, strongly suggesting that the 6-TG that is incorporated into DNA is responsible for this sensitization.

Sulforaphane protects 6-thioguanine-treated keratinocytes against the damaging effects of UVA radiation

To test whether SF protects keratinocytes against oxidative stress caused by the combination of 6-TG and UVA radiation, we used the established murine keratinocyte cell line Kera-308 (48) since primary keratinocytes do not proliferate in the absence of growth factors, and consequently do not incorporate 6-TG into their DNA. In this cell line, the SF treatment resulted in ~50% reduction in the formation of ROS in comparison with cells that had not been treated with SF (Figure 4D). The levels of GSH were increased by ~3-fold by the SF treatment (Figure 4E), and those of NQO1 by >4-fold (Figure 4F). Interestingly, similar to the experiment in primary keratinocytes in the absence of 6-TG (Figure 3F), exposure to UVA radiation in the presence of 6-TG also led to a decrease in NQO1 activity (Figure 4F), further supporting the notion that the enzyme was not fully functional in the highly oxidative environment produced by the combination of 6-TG and UVA radiation.

Protective effects of sulforaphane are due to upregulation of Nrf2-dependent cytoprotective responses

We then investigated the mechanism(s) by which SF protected against oxidative stress caused by the combination of 6-TG and UVA radiation. Because SF is not redox-active and was no longer present at the time of irradiation due to its relatively short half-life (in the order of a few hours) (49) its protective effects are most probably due to

its indirect antioxidant activity, i.e. the Nrf2-dependent upregulation of cytoprotective proteins. To test this possibility, we used MEFs isolated from wild-type or Nrf2-knockout mice. As predicted from the experiments described above, the degree of 6-TG-mediated sensitization to oxidative stress caused by UVA radiation is proportional to the extent of 6-TG incorporation in DNA (Figure 5A). Therefore, to be able to compare directly the protective effect of sulforaphane in the two different cell lines (i.e. wild-type and Nrf2-knockout MEFs), we first adjusted the experimental conditions to such that resulted in similar levels of 6-TG incorporation in their genomic DNA. Thus, we found that ~5–6% of dG in DNA was substituted with 6-TG when wild-type and Nrf2-knockout MEFs were exposed for 24 h to 1 or 0.5 µM 6-TG in the cell culture medium, respectively (Figure 5B, white bars). Notably, this requirement for different 6-TG concentrations in the cell culture medium resulting in similar 6-TG incorporation in DNA can be attributed to the differences in growth rates between the cells of the two genotypes. We then asked whether exposure of the MEFs to SF affected the 6-TG incorporation in DNA. We found that the levels of 6-TG in DNA were unaltered by the SF treatment in either wild-type or Nrf2-knockout MEFs (Figure 5B, compare white and black bars). This allowed us to evaluate directly the role of Nrf2 in the protective effect of SF under conditions of equal 6-TG DNA incorporation between SF-treated and acetonitrile-treated control cells.

In full agreement with the results for the primary dermal fibroblasts, when MEFs were treated with 6-TG for 24 h and then exposed to UVA radiation, the levels of ROS were increased by 4-fold compared with the ROS levels in cells that were irradiated but not exposed to 6-TG (Figure 6A). Similar to the protection afforded by SF in dermal fibroblasts, treatment of wild-type MEFs with the isothiocyanate led to a significant ~35% reduction ($P < 0.01$) in the formation of ROS in comparison with MEFs that had not been treated with SF. In sharp contrast with wild-type cells, the protective effect of SF was completely absent in Nrf2-knockout MEFs (Figure 6B). Consistent with the Nrf2 status and its stabilization by SF (Figure 6C), in wild-type sham-irradiated cells, the NQO1 enzyme activity was induced by ~2-fold by SF treatment, whereas it was low and uninducible in Nrf2-knockout MEFs (Figure 6D). The levels of GSH were then determined in a parallel experiment. Compared with cells that were treated with the acetonitrile control, the levels of GSH were ~2-fold higher ($P < 0.001$) in SF-treated UVA-irradiated wild-type MEFs, and remained high following the combined exposure to 6-TG and UVA radiation (Figure 6E, white bars). In agreement with the lack of protection against ROS formation under conditions of Nrf2 deficiency, SF was unable to upregulate the levels of GSH in the Nrf2-knockout MEFs. Furthermore, in the absence of Nrf2, exposure to SF lowered the GSH levels even further, and did not protect against the UVA-mediated depletion of GSH either in the absence or in the presence of 6-TG (Figure 6E, black bars). These results imply that the protective effect of SF against oxidative stress caused by UVA radiation both under basal conditions as well as after treatment with 6-TG is due to its ability to induce Nrf2-dependent cytoprotective responses.

Conclusions

Treatment with 6-TG, a surrogate for the immunosuppressive and anti-inflammatory agent azathioprine, leads to profound sensitization to oxidative stress and glutathione depletion upon exposure to UVA radiation, the damaging effects of which are mediated by generation of ROS. The extent of sensitization is greatest for spectral wavelength at which 6-TG absorbs, and is dependent on treatment duration and the level of guanine substitution with 6-TG, strongly suggesting that sensitization is mainly due to the 6-TG that is incorporated in genomic DNA. SF provided protection at all doses of UVA radiation tested (up to 20 J/cm^2) under both basal conditions and after 6-TG treatment. Protection correlates with increased levels of NQO1 and GSH, and requires transcription factor Nrf2. In contrast with the
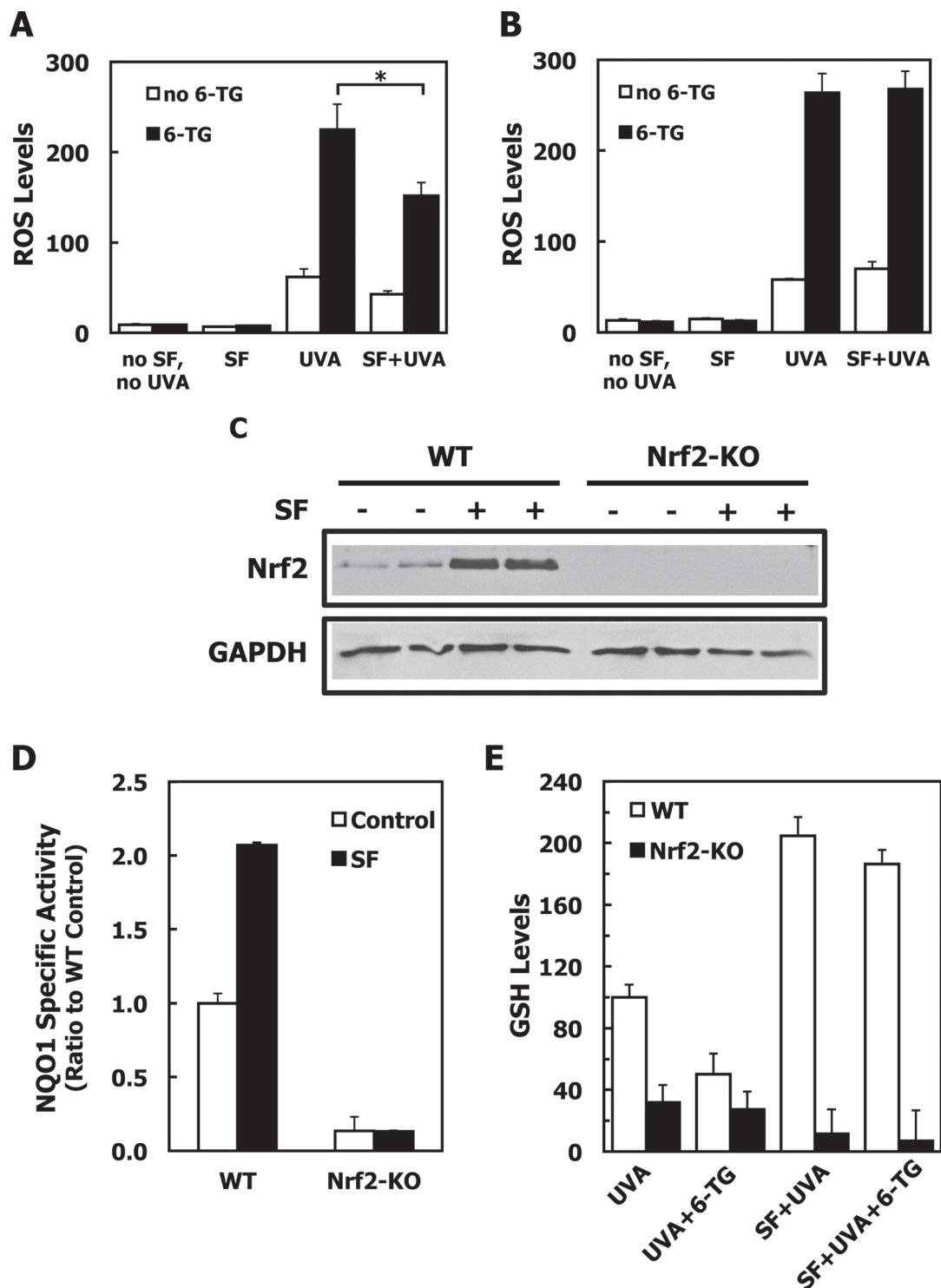
Fig. 6. Sulforaphane protects wild-type, but not Nrf2-knockout, 6-TG-treated mouse embryonic fibroblast (MEFs) against UV radiation-induced oxidative stress. (**A** and **B**) MEFs were plated at 250 000 cells per well in 6-well plates. Seven hours later, they were exposed to either solvent (0.1% acetonitrile), or 3 µM SF for a further 17 h. Cells were then treated with either solvent (0.00005 N NaOH) or 1 µM 6-TG (WT MEFs, panel A) or 0.5 µM 6-TG (Nrf2-knockout MEFs, panel B). After 24 h, cells were washed with HBSS, and exposed to UVA (3 J/cm^2) in 1.0 ml of HBSS. ROS generated by the UV radiation were quantified by the probe 2′,7′-dichlorodihydrofluorescein diacetate and fluorescence intensity was measured 1 h postirradiation. (**C**) WT (lanes 1–4) or Nrf2-knockout (lanes 5–8) MEFs (1.5 × 10^6 per dish) were plated on 10 cm dishes. Twenty four hours later, they were exposed to either solvent (0.1% acetonitrile, lanes 1, 2, 5 and 6), or 3 µM SF (lanes 3, 4, 7 and 8) for a further 3 h. The levels of Nrf2 were determined in whole-cell lysates by western blotting. (**D**) NQO1 enzyme activity was measured in lysates prepared from sham-irradiated control cells from the experiment described in A and B. Data are expressed as ratio of wild-type untreated cells. (**E**) GSH levels were determined in a parallel experiment 2 h after irradiation. Data are expressed as the percentage of wild-type, UVA-irradiated cells. For all panels, mean ± SD are shown (n = 3). P values were calculated by Student's t-test (*P < 0.01). Results are representative of three independent experiments. WT, wild-type; Nrf2-KO, Nrf2-knockout cells.

protective effect against UVA radiation, under our experimental conditions, the isothiocyanate did not protect against direct DNA damage caused by UVB radiation, implicating the indirect antioxidant activity of SF, via induction of Nrf2-dependent genes, as the major protective mechanism. Notably, in addition to protection in primary cells, we also observed a strong protective effect by SF in Kera-308 cells that harbour constitutively active RAS oncogene and are able to form papillomas in skin grafts on athymic nude mouse hosts (48). This finding suggests that an extreme caution should be taken when designing dosing regiments for chemoprotection as induction of Nrf2 may promote tumor development under conditions of constitutive oncogene activation, and may even contribute to drug resistance (50–52). Nonetheless, previous studies have shown that topical (i.e. SF-containing broccoli sprout extracts) or oral (i.e. glucoraphanin-rich broccoli sprout extracts) SF treatments reduce tumor development after a chronic schedule of UV radiation (16,53). Taken together, these data provide strong support for the view that SF, and other inducers of the Nrf2 pathway, protect against UV radiation-induced skin damage primarily by reducing oxidative stress. Because SF-rich broccoli sprout preparations are currently under investigation in numerous human studies (21), our findings encourage future clinical trials in patients at high risk for photodamage and photocarcinogenesis of the skin, such as those who are undergoing long-term thiopurine therapies.

References

1. Alam,M. *et al.* (2001) Cutaneous squamous-cell carcinoma. *N. Engl. J. Med.*, **344**, 975–983.
2. Proby,C.M. *et al.* (2009) The epidemiology of transplant-associated keratinocyte cancers in different geographical regions. *Cancer Treat. Res.*, **146**, 75–95.
3. Clydesdale,G.J. *et al.* (2001) Ultraviolet light induced injury: immunological and inflammatory effects. *Immunol. Cell Biol.*, **79**, 547–568.
4. Svobodova,A. *et al.* (2006) Ultraviolet light induced alteration to the skin. *Biomed. Pap. Med. Fac. Univ. Palacky. Olomouc. Czech. Repub.*, **150**, 25–38.
5. Terui,T. *et al.* (2001) Molecular events occurring behind ultraviolet-induced skin inflammation. *Curr. Opin. Allergy Clin. Immunol.*, **1**, 461–467.
6. Young,A.R. (2006) Acute effects of UVR on human eyes and skin. *Prog. Biophys. Mol. Biol.*, **92**, 80–85.
7. Karran,P. *et al.* (2008) Thiopurines in current medical practice: molecular mechanisms and contributions to therapy-related cancer. *Nat. Rev. Cancer*, **8**, 24–36.
8. Gueranger,Q. *et al.* (2011) Crosslinking of DNA repair and replication proteins to DNA in cells treated with 6-thioguanine and UVA. *Nucleic Acids Res.*, **39**, 5057–5066.
9. Perrett,C.M. *et al.* (2008) Azathioprine treatment photosensitizes human skin to ultraviolet A radiation. *Br. J. Dermatol.*, **159**, 198–204.
10. Huang,C.C. *et al.* (2005) Protective effects of (–)-epicatechin-3-gallate on UVA-induced damage in HaCaT keratinocytes. *Arch. Dermatol. Res.*, **296**, 473–481.
11. Sies,H. *et al.* (2004) Carotenoids and UV protection. *Photochem. Photobiol. Sci.*, **3**, 749–752.
12. Dinkova-Kostova,A.T. *et al.* (2008) Direct and indirect antioxidant properties of inducers of cytoprotective proteins. *Mol. Nutr. Food Res.*, **52 (Suppl. 1)**, S128–S138.
13. Talalay,P. (2000) Chemoprotection against cancer by induction of phase 2 enzymes. *Biofactors*, **12**, 5–11.
14. Zhang,Y. *et al.* (1992) A major inducer of anticarcinogenic protective enzymes from broccoli: isolation and elucidation of structure. *Proc. Natl. Acad. Sci. U.S.A.*, **89**, 2399–2403.
15. Dinkova-Kostova,A.T. *et al.* (2005) The role of Keap1 in cellular protective responses. *Chem. Res. Toxicol.*, **18**, 1779–1791.
16. Dinkova-Kostova,A.T. *et al.* (2006) Protection against UV-light-induced skin carcinogenesis in SKH-1 high-risk mice by sulforaphane-containing broccoli sprout extracts. *Cancer Lett.*, **240**, 243–252.
17. Kerns,M.L. *et al.* (2007) Reprogramming of keratin biosynthesis by sulforaphane restores skin integrity in epidermolysis bullosa simplex. *Proc. Natl. Acad. Sci. U.S.A.*, **104**, 14460–14465.
18. Talalay,P. *et al.* (2007) Sulforaphane mobilizes cellular defenses that protect skin against damage by UV radiation. *Proc. Natl. Acad. Sci. U.S.A.*, **104**, 17500–17505.
19. Saw,C.L. *et al.* (2011) Impact of Nrf2 on UVB-induced skin inflammation/photoprotection and photoprotective effect of sulforaphane. *Mol. Carcinog.*, **50**, 479–486.
20. Juge,N. *et al.* (2007) Molecular basis for chemoprevention by sulforaphane: a comprehensive review. *Cell. Mol. Life Sci.*, **64**, 1105–1127.
21. Dinkova-Kostova,A.T. *et al.* (2012) Glucosinolates and isothiocyanates in health and disease. *Trends Mol. Med.*, **18**, 337–347.
22. Heiss,E. *et al.* (2001) Nuclear factor kappa B is a molecular target for sulforaphane-mediated anti-inflammatory mechanisms. *J. Biol. Chem.*, **276**, 32008–32015.
23. Cheung,K.L. *et al.* (2010) Molecular targets of dietary phenethyl isothiocyanate and sulforaphane for cancer chemoprevention. *AAPS J.*, **12**, 87–97.
24. Healy,Z.R. *et al.* (2011) Inactivation of tautomerase activity of macrophage migration inhibitory factor by sulforaphane: a potential biomarker for anti-inflammatory intervention. *Cancer Epidemiol. Biomarkers Prev.*, **20**, 1516–1523.
25. Al-Abed,Y. *et al.* (2005) ISO-1 binding to the tautomerase active site of MIF inhibits its pro-inflammatory activity and increases survival in severe sepsis. *J. Biol. Chem.*, **280**, 36541–36544.
26. Leng,L. *et al.* (2003) MIF signal transduction initiated by binding to CD74. *J. Exp. Med.*, **197**, 1467–1476.
27. Wang,F. *et al.* (2011) Macrophage migration inhibitory factor activates cyclooxygenase 2-prostaglandin E2 in cultured spinal microglia. *Neurosci. Res.*, **71**, 210–218.
28. Mahéo,K. *et al.* (1997) Inhibition of cytochromes P-450 and induction of glutathione S-transferases by sulforaphane in primary human and rat hepatocytes. *Cancer Res.*, **57**, 3649–3652.
29. Gross-Steinmeyer,K. *et al.* (2010) Sulforaphane- and phenethyl isothiocyanate-induced inhibition of aflatoxin B1-mediated genotoxicity in human hepatocytes: role of GSTM1 genotype and CYP3A4 gene expression. *Toxicol. Sci.*, **116**, 422–432.
30. Hu,R. *et al.* (2006) Gene expression profiles induced by cancer chemopreventive isothiocyanate sulforaphane in the liver of C57BL/6J mice and C57BL/6J/Nrf2 (-/-) mice. *Cancer Lett.*, **243**, 170–192.
31. Kwak,M.K. *et al.* (2007) Role of increased expression of the proteasome in the protective effects of sulforaphane against hydrogen peroxide-mediated cytotoxicity in murine neuroblastoma cells. *Free Radic. Biol. Med.*, **43**, 809–817.
32. Gan,N. *et al.* (2010) Sulforaphane activates heat shock response and enhances proteasome activity through up-regulation of Hsp27. *J. Biol. Chem.*, **285**, 35528–35536.
33. Jackson,S.J. *et al.* (2004) Sulforaphane inhibits human MCF-7 mammary cancer cell mitotic progression and tubulin polymerization. *J. Nutr.*, **134**, 2229–2236.
34. Jackson,S.J. *et al.* (2004) Sulforaphane: a naturally occurring mammary carcinoma mitotic inhibitor, which disrupts tubulin polymerization. *Carcinogenesis*, **25**, 219–227.
35. Myzak,M.C. *et al.* (2004) A novel mechanism of chemoprotection by sulforaphane: inhibition of histone deacetylase. *Cancer Res.*, **64**, 5767–5774.
36. Park,S.Y. *et al.* (2007) Induction of apoptosis by isothiocyanate sulforaphane in human cervical carcinoma HeLa and hepatocarcinoma HepG2 cells through activation of caspase-3. *Oncol. Rep.*, **18**, 181–187.
37. Bertl,E. *et al.* (2006) Inhibition of angiogenesis and endothelial cell functions are novel sulforaphane-mediated mechanisms in chemoprevention. *Mol. Cancer Ther.*, **5**, 575–585.

38. Kawachi,Y. *et al.* (2008) Attenuation of UVB-induced sunburn reaction and oxidative DNA damage with no alterations in UVB-induced skin carcinogenesis in Nrf2 gene-deficient mice. *J. Invest. Dermatol.*, **128**, 1773–1779.

39. Kimura,S. *et al.* (2009) Essential role of Nrf2 in keratinocyte protection from UVA by quercetin. *Biochem. Biophys. Res. Commun.*, **387**, 109–114.

40. Gao,X. *et al.* (2001) Powerful and prolonged protection of human retinal pigment epithelial cells, keratinocytes, and mouse leukemia cells against oxidative damage: the indirect antioxidant effects of sulforaphane. *Proc. Natl. Acad. Sci. U.S.A.*, **98**, 15221–15226.

41. Kalra,S. *et al.* (2011) Oral azathioprine leads to higher incorporation of 6-thioguanine in DNA of skin than liver: the protective role of the Keap1/Nrf2/ARE pathway. *Cancer Prev. Res. (Phila).*, **4**, 1665–1674.

42. Lichti,U. *et al.* (2008) Isolation and short-term culture of primary keratinocytes, hair follicle populations and dermal cells from newborn mice and keratinocytes from adult mice for *in vitro* analysis and for grafting to immunodeficient mice. *Nat. Protoc.*, **3**, 799–810.

43. Fahey,J.W. *et al.* (2004) The 'Prochaska' microtiter plate bioassay for inducers of NQO1. *Meth. Enzymol.*, **382**, 243–258.

44. Prochaska,H.J. *et al.* (1988) Direct measurement of NAD(P)H:quinone reductase from cells cultured in microtiter wells: a screening assay for anti-carcinogenic enzyme inducers. *Anal. Biochem.*, **169**, 328–336.

45. O'Donovan,P. *et al.* (2005) Azathioprine and UVA light generate mutagenic oxidative DNA damage. *Science*, **309**, 1871–1874.

46. McMahon,M. *et al.* (2003) Keap1-dependent proteasomal degradation of transcription factor Nrf2 contributes to the negative regulation of antioxidant response element-driven gene expression. *J. Biol. Chem.*, **278**, 21592–21600.

47. Hirota,A. *et al.* (2005) Ultraviolet A irradiation induces NF-E2-related factor 2 activation in dermal fibroblasts: protective role in UVA-induced apoptosis. *J. Invest. Dermatol.*, **124**, 825–832.

48. Strickland,J.E. *et al.* (1988) Development of murine epidermal cell lines which contain an activated rasHa oncogene and form papillomas in skin grafts on athymic nude mouse hosts. *Cancer Res.*, **48**, 165–169.

49. Ye,L. *et al.* (2001) Total intracellular accumulation levels of dietary isothiocyanates determine their activity in elevation of cellular glutathione and induction of Phase 2 detoxification enzymes. *Carcinogenesis*, **22**, 1987–1992.

50. DeNicola,G.M. *et al.* (2011) Oncogene-induced Nrf2 transcription promotes ROS detoxification and tumorigenesis. *Nature*, **475**, 106–109.

51. Sporn,M.B. *et al.* (2012) NRF2 and cancer: the good, the bad and the importance of context. *Nat. Rev. Cancer*, **12**, 564–571.

52. Xu,T. *et al.* (2012) Dual roles of sulforaphane in cancer treatment. *Anticancer Agents Med. Chem.* In press.

53. Dinkova-Kostova,A.T. *et al.* (2010) Dietary glucoraphanin-rich broccoli sprout extracts protect against UV radiation-induced skin carcinogenesis in SKH-1 hairless mice. *Photochem. Photobiol. Sci.*, **9**, 597–600.